

# All-Lignin Polyelectrolyte Multilayers as Renewable and Biodegradable Nanofiltration Membranes

Tjerk R. Watt, Stefan Peil, Wendy A. Jonkers, Jurjen A. Regenspurg, Frederik R. Wurm,\* and Wiebe M. de Vos\*



Cite This: *ACS Appl. Polym. Mater.* 2023, 5, 8547–8558



Read Online

ACCESS |



Metrics & More



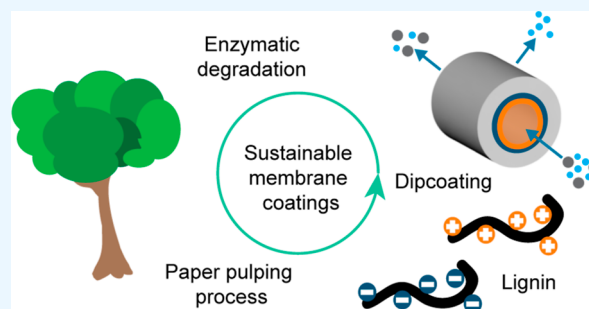
Article Recommendations



Supporting Information

**ABSTRACT:** Polyelectrolyte multilayers have proven to be versatile materials for the fabrication of nanofiltration membranes with a wide range of properties and applications. A problem of these membranes is that they are made of nonrenewable and nonbiodegradable fossil resources, rendering them unsustainable for the future. To solve this, we present lignin as a renewable and biodegradable alternative for the fabrication of polyelectrolyte multilayer membranes (PEMMs). Here, lignosulfonate was used as a polyanion in combination with modified Kraft lignin as a polycation in a layer-by-layer self-assembly process to coat hollow fiber support membranes to obtain so-called all-lignin PEMMs. The PEMMs showed loose nanofiltration properties (molecular weight cutoff > 1 kDa, MgSO<sub>4</sub> retention 20%) that could easily be fine-tuned by changing the ionic strength of the coating solutions. Furthermore, the lignin PEMMs have excellent stability in saline solutions of up to 5 M NaCl and were stable in a pH range from 1 to 11. Additionally, the lignin retained its biodegradable properties in the presence of laccase enzymes after forming a PEMM. Our results indicate that lignins are a suitable candidate for replacing fossil-based polyelectrolytes for the fabrication of chemically stable, renewable, and biodegradable PEMMs.

**KEYWORDS:** layer-by-layer, biopolymer, lignosulfonate, membrane stability, renewables



## INTRODUCTION

Natural organic matter (NOM) is a mixture of complex organic compounds present in aquatic environments that are known to create problems in drinking water treatment plants.<sup>1–3</sup> In the past few decades, the concentration of NOMs have been increasing in surface waters all over the world to such an extent that conventional water treatments such as coagulation fail to sufficiently remove these NOMs in some cases.<sup>4–6</sup> Therefore, in recent years, wastewater treatment plants have looked toward nanofiltration (NF) membranes for the removal of NOMs due to their ability to selectively remove small organic compounds while retaining a good permeability toward ions needed for drinking water.<sup>2,3</sup> Especially, hollow fiber (HF) NF membranes are looked to for this task due to their stability against the physical cleaning required to remove the membrane fouling that NOMs cause.<sup>7,8</sup>

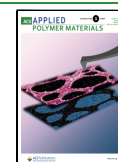
One of the HF membrane types that is currently being used commercially for such applications is the polyelectrolyte multilayer membrane (PEMM).<sup>2,9,10</sup> PEMMs are prepared by coating a charged ultrafiltration support membrane alternately with positively charged polyelectrolytes (polycations) and negatively charged polyelectrolytes (polyanions) to form a polyelectrolyte multilayer (PEM) that fully covers the porous support.<sup>10,11</sup> Using this layer-by-layer (LbL) self-assembly method, an active separation layer with well-defined

thickness can be formed.<sup>10</sup> The membrane then obtains the mechanical strength of the thicker substrate while keeping the good selectivity and high permeability of the PEM due to its dense, but thin, structure.<sup>11</sup> The selectivity of these PEMMs can be easily controlled during the fabrication process. By changing parameters such as the salt concentration or pH of the coating solution, the type of polyelectrolyte, and the number of layers coated, among others, the density and, therefore, the selectivity of the resulting PEMM can be fine-tuned.<sup>10,12</sup> On comparing PEMMs to other thin film composite membranes such as those prepared through interfacial polymerization (IP), the PEMMs are found to have some clear advantages over the IP-based membranes. The LbL technique used to fabricate PEMMs is considered to be a green and sustainable method due to only water being required as a solvent,<sup>13,14</sup> and the LbL technique can be more easily applied to substrates with more complex geometries such as the HF geometry so as to be able to utilize all the advantages

**Received:** July 24, 2023

**Accepted:** September 18, 2023

**Published:** September 28, 2023



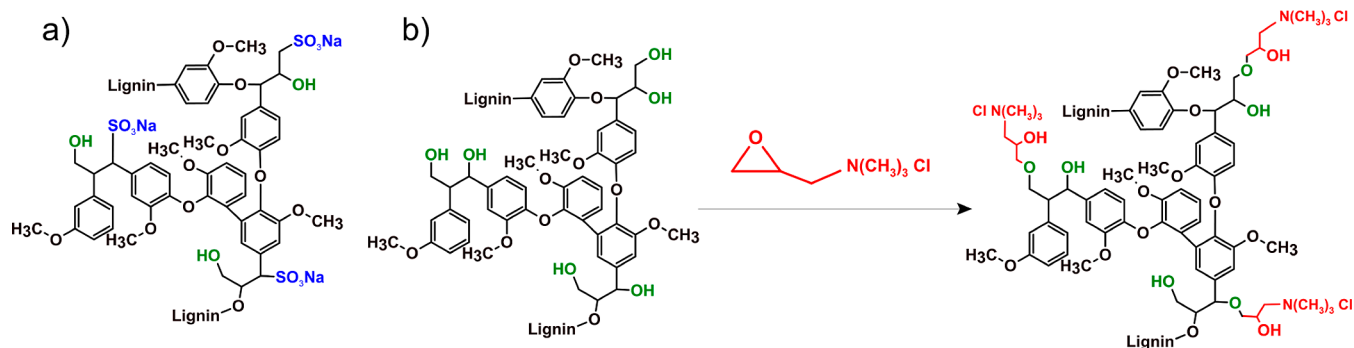


**Figure 1.** (a) Representative structure of lignosulfonate; (b) modification reaction of Kraft lignin with GTAC.

that the HF geometry brings with it, such as their resistance to physical cleaning and their self-supporting structure, among others.<sup>7,14</sup> Due to the tunable separation properties in the NF range and their simple fabrication method, PEMMs have become an attractive option for water filtration applications, including for the complex problem of NOM removal.<sup>9,10</sup>

One of the downsides of these membranes is that most PEMMs are, currently, made with limited and nonbiodegradable resources, such as polymers synthesized from fossil-based materials.<sup>10,15,16</sup> Therefore, even though the LbL fabrication process used for PEMMs is seen as a green and sustainable method, because it only requires water as a solvent,<sup>13</sup> these PEMMs cannot be considered as a sustainable solution for water shortages and the removal of organic solutes such as NOMs. Thus, a solution to this problem would be to replace the nonbiodegradable and nonrenewable polymers that are currently being used with renewable and biodegradable alternatives. Ideally, here, the support membrane should also be prepared from renewable and biodegradable polymers; such membranes are already being investigated.<sup>17</sup>

One relevant polymer that could form such a sustainable PEMM would be lignin. Lignin is a nontoxic and renewable polymer originating from the cell walls of plants.<sup>18</sup> It is the second most abundant biopolymer on earth and is produced through the pulping process in the paper industry, where the yearly production is estimated to be  $1.5 \times 10^{11}$  tonnes.<sup>19</sup> Currently, it is being treated as a waste product and being burnt off for heat recovery, making it a cheap and widely available resource for other applications.<sup>18–20</sup> Furthermore, lignin with different chemical structures can be obtained depending on the type of pulping process used. Two of these types of pulping process are the sulfite process and the Kraft process.<sup>19</sup> The sulfite process produces lignin with sulfate groups attached to its structure, making these so-called lignosulfonates water-soluble polyanions ideal for coating PEMs (Figure 1a). The Kraft process produces lignin that dissolves in water under alkaline conditions. This Kraft lignin can, however, easily be modified by reacting its hydroxyl groups with glycidyltrimethylammonium chloride (GTAC) to obtain ammonium groups that turn the lignin into a polycation soluble in water at neutral pHs (Figure 1b), ideal for coating PEMs.<sup>21–23</sup> Next to this, lignin is stable under hydrolytic conditions due to its aromatic structure,<sup>24</sup> making it a relatively stable polymer for water filtration applications. However, it can still be biodegraded by enzymes under the right conditions.<sup>18,25–27</sup> These aspects indicate that lignin is an ideal candidate to act as a renewable and biodegradable polyelectrolyte in PEMMs, and their use in the membrane

separation industry can be considered an important step forward toward a circular economy.

In previous research performed with this polyelectrolyte pair,<sup>21</sup> it was proven that the cationic Kraft lignin and lignosulfonates are capable of forming PEM capsules, which can hold spores. These capsules retained their enzymatic biodegradability. However, modified species of lignin such as Kraft lignin and lignosulfonates are harder to degrade due to their chemical modification varying from that of pristine lignin in nature.<sup>28</sup> Next to this, PEMMs have already been fabricated using lignin as one of the polyelectrolytes. Lignosulfonates have been used in combination with synthetic polycations in the fabrication of a PEMM for the removal of tri- and tetravalent ions,<sup>29</sup> while unmodified Kraft lignin has also been used in combination with synthetic polycations to form a PEM to act as an antifouling coating for ultrafiltration (UF) membranes used in oil separations.<sup>30</sup> However, no cationic lignin has ever been used in the fabrication of a PEMM. Thus, no all-lignin PEMM has ever been made to obtain a PEMM made from renewable and biodegradable resources.

Therefore, to determine if lignin can act as a renewable and biodegradable alternative resource in the application of aqueous filtration using NF membranes, we used lignosulfonate and modified cationic Kraft lignin as a membrane material to coat a poly(ether sulfonate) (PES) hollow fiber UF support membrane to form the first all-lignin PEMM. We measured the permeability,  $\text{MgSO}_4$  retention, and 90% molecular weight cutoff (MWCO) of the membranes in a crossflow setup. Next to this, the stability of the membranes in saline, acidic, and basic environments was determined through overnight treatment with solutions of different salinity or pH. Finally, the biodegradability of the PEMMs was tested by treating the membranes with a laccase enzyme solution to assess the biodegradability of the lignin. The results show that lignin is a suitable material for the fabrication of PEMMs with desirable separation properties, excellent chemical stabilities, and saline stabilities beyond that of synthetic polyelectrolytes while still being biodegradable in the presence of specific enzymes. Our all-lignin PEMMs thus set the basis for the development of renewable and biodegradable nanofiltration membranes.

## EXPERIMENTAL SECTION

**Materials.** Sodium chloride (NaCl) (pharmaceutical quality 99.96%) was obtained from Nouryon; sodium lignosulfonate (TCl, product #L0098, batch #V3G6G, see Supporting Information S1 for the characterization of the lignosulfonate) and glycidyltrimethylammonium chloride solution (GTAC, 80% in water) were obtained from TCl; PES hollow fibers (a MWCO of 10 kDa, an inner diameter of 0.7 mm with a negatively charged separation skin, and a permeability

of 142.8 L/h  $\times$  m<sup>2</sup>) provided by NX filtration B.V., Enschede, The Netherlands, were used as supports; magnesium sulfonate heptahydrate (MgSO<sub>4</sub>,  $\geq 99.0\%$ ), polyethylenimine (PEI, MW = 25 000 g/mol), hydrochloric acid solution (HCl, 37% ACS Reagent), sodium hydroxide (NaOH, pellets), 2-chloro-4,4,5,5-tetramethyl-1,3,2-dioxaphospholane (95%), Kraft lignin (Lignin, alkali, Lot:#MKBV5831 V), laccase from *Trametes versicolor* fungus (0.89 U/mg), sodium azide (NaN<sub>3</sub>, 99.5%), and deuterated chloroform (CDCl<sub>3</sub>, 99.9%) were obtained from Sigma-Aldrich; endo-*N*-hydroxy-5-norbornene-2,3-dicarboximide 97% was obtained from Alfa Aesar; glycerol (85% aqueous solution), sulfuric acid (95–97%), acetic acid (99.8%), and polyethylene glycol (PEG) (MW 200, 400, 1000, 1500, 2000, 3000, 4000, 6000, and 10 000) were obtained from Merck; deuterium oxide (D<sub>2</sub>O, 99.9%) and pyridine-*d*<sub>5</sub> (99.5%) were obtained from Deutero GmbH; Cr(III)acetylacetonate (97%) was obtained from Acros organics; 2,2'-azino-bis(3-ethylbenzothiazoline-6-sulfonic acid) diammonium salt (ABTS) was obtained from Roche Diagnostics GmbH; and sodium acetate (99.0%) was obtained from Fluka. The water used in this research was obtained using a Milli-Q Ultrapure water purification system. 2-Propanol (IPA, technical grade) was obtained from Boom.

**Synthesis of Cationic Lignin.** For the synthesis of cationic lignin, the procedure from the study by Peil et al.<sup>21</sup> was used (Figure 1b). One g portion of Kraft lignin was dissolved into a 0.2 M NaOH aqueous solution to obtain a 1 wt % solution of Kraft lignin. GTAC was added in a molar ratio of 1:2 (OH groups to GTAC) as determined from <sup>31</sup>P NMR according to the method of Balakshin and Capanema<sup>31</sup> (Supporting Information S1). The reaction mixture was stirred at 100 rpm for 1 h at 70 °C. Afterward, the mixture was neutralized by adding a 10 wt % solution of sulfuric acid followed by a dialysis against 3 L of deionized water (DI water) for 3 days to remove the excess GTAC and low-molecular weight lignin fractions. A Spectra/Por 7 dialysis membrane made of regenerated cellulose with a MWCO of 1 kDa was used for the dialysis. The water was replaced twice a day. Afterward, cationic lignin was extracted from the dialyzed product and separated from the remaining insoluble lignin fraction; thereafter, the dialyzed product was transferred to centrifuge vials, washed three times with 300 mL of DI water, and centrifuged (15 min, 10 000 rcf) until the supernatant did not show any brown color. The remaining insoluble particles in the supernatant were removed via suction filtration (filter paper: VOS instrumenten VOS-23015, 20–25  $\mu$ m pore size). Then, the volume of the filtrate was reduced by heating the solution to 50 °C in a beaker and blowing a stream of air over the surface. After the volume was reduced to approximately 50 mL, the solution was freeze-dried and 0.5 g of water-soluble cationic lignin was obtained. The cationic lignin was then characterized through Fourier transform infrared spectroscopy (FTIR) and proton nuclear magnetic resonance spectroscopy (<sup>1</sup>H NMR) (see Supporting Information S1 for the methods and results). Although this article aims to prove that lignin can act as a sustainable alternative to synthetic polyelectrolytes, the authors acknowledge that this modification cannot be considered sustainable. Although the solvent used is sustainable, the GTAC is a highly toxic chemical with long-lasting environmental effects.<sup>32</sup> The authors would therefore like to emphasize the need for further research into a sustainable synthesis for the production of water-soluble cationic lignin.

**Multilayer Growth Characterization. Reflectometry.** Fixed-angle optical reflectometry was performed to study the growth of the lignin PEMs. During the reflectometry measurements, a silica wafer with an 82 nm thick negatively charged SiO<sup>-</sup> surface was used as the substrate for the growth of the lignin PEMs. The wafer was cleaned before the measurement with water and ethanol, after which it was dried under a nitrogen stream and cleaned with O<sub>2</sub> plasma for 10 min at an O<sub>2</sub> pressure of 0.45 mbar (Femto-Diener electronic plasma cleaner at 100% power). During the measurements, the wafer was placed into a cell in which a 0.1 g/L solution of PEI containing 5 mM NaCl was introduced (PEI is used here to form a defect-free bottom layer<sup>33</sup>). Then, when the reflectometer showed that no more PEI was being adsorbed, a rinsing solution consisting of Milli-Q water with 5 mM NaCl was introduced to wash away the excess PEI adsorbed to

the wafer. After this initial layer of PEI was grown, a 0.1 g/L lignosulfonate solution containing 5 mM NaCl was introduced into the cell, followed by another rinsing step, a 0.1 g/L cationic lignin solution containing 5 mM NaCl, and another rinsing step to form one lignin bilayer on top of the PEI monolayer. This cycle was repeated until 4.5 bilayers of lignin were grown on top of the PEI monolayer to form 5 bilayers of polyelectrolyte on top of the wafer. During the growth of the bilayers, a monochromatic He–Ne laser with a wavelength of 632.8 nm was directed at the wafer under an angle of 71° (the Brewster angle of silica). The light of the laser was then reflected off of the sample surface toward a detector that measured the reflectance of the parallel polarized light ( $R_p$ ) and perpendicular polarized light ( $R_s$ ) components. The reflectometer expressed these reflectances as the ratio between the two components ( $R_p/R_s$ ), defined as component *S*. The initial ratio  $S_0$  and its change ( $\Delta S$ ) show a linear dependence with the mass of adsorbed polyelectrolytes, in mg/m<sup>2</sup>, according to eq 1.<sup>34</sup>

$$\Gamma = Q \cdot \frac{\Delta S}{S_0} \quad (1)$$

Here, *Q* is the sensitivity factor (*Q*-factor) of the system and  $\Gamma$  is the adsorption in mg/m<sup>2</sup>.

Using the *Q*-factors for both lignosulfonate and the cationic lignin, 21 and 24 mg/m<sup>2</sup> respectively (Supporting Information S2), and eq 1 the absorbed mass of lignin was then calculated from the measured change in the ratio of polarized light ( $\Delta S$ ). The reflectometry measurements were repeated using 50 and 500 mM concentrations of NaCl in the coating and rinsing solutions to study the influence of the ionic strength on the growth of the multilayers. The layers were grown onto the silica wafer three times in order to determine the standard deviation.

**Membrane Fabrication.** PEM membranes were created through the dip-coating process. Lignosulfonate and cationic lignin were used as polyelectrolytes. Negatively charged PES hollow fiber UF membranes were used as supports. First, the supports were cleaned by leaving them in a 10 wt % ethanol–water solution overnight to remove the protective glycerol coating filling the pores. For the dip-coating process, two sets of five solutions were made by dissolving NaCl into milli-Q water to create either 5, 50, or 500 mM NaCl solutions. To two solutions of each set was added either lignosulfonate or cationic lignin to obtain a concentration of 0.1 g/L. The pH of the lignin solutions was measured with a pH meter (Mettler Toledo FiveEasy Plus pH meter) and adjusted with NaOH and HCl solutions to obtain a pH of 6. The dip-coating was performed by dipping the supports in each of the three NaCl solutions for 5 min each to rinse the substrate, after which the fibers were dipped for 15 min in the cationic lignin solution. Next, the 3 rinsing steps were repeated before the substrates were dipped into the lignosulfonate solution for 15 min to form 1 bilayer. After coating the desired amount of bilayers, the membranes were left in an aqueous solution containing 15 wt % glycerol overnight, after which the membranes were left to dry overnight. The dried membranes were potted into modules by putting them into separate 24 cm long polyethylene tubes and gluing them into place by injecting Bison polyurethane 2 component glue at the ends of the tube. The glue was then left to harden overnight. For each different membrane type, 4 membranes were fabricated, so the standard deviation could be determined.

**Membrane Characterization.** Pure water permeability, salt retention, MWCO, and salt stability measurements were all performed using a home-built crossflow setup. The details of this setup have been accurately described by Elshof et al.<sup>35</sup> In the crossflow setup, the fibers were operated in the bore-side feed mode. The temperature of the feed was kept at 20 °C, and the feed was operated at a flow rate of 20 L/h (corresponding to a laminar flow profile) and an average membrane pressure of 2.0 bar. Before any characterization steps, the new membranes were flushed with Milli-Q water for half an hour in the crossflow setup to remove the glycerol.

**Pure Water Permeability.** The pure water permeability of the membranes was measured by using Milli-Q water as a feed. The permeate was collected over half an hour and weighed. The pure water permeability was then calculated using eq 2.<sup>36</sup>

$$Pe = \frac{m}{t \times P \times d_i \times l \times \pi} \quad (2)$$

Here,  $Pe$  is the permeability in  $L/(\text{bar} \times \text{h} \times \text{m}^2)$ ;  $t$  the time of the experiment in hours;  $P$  the average pressure over the membrane in bar;  $d_i$  the inner diameter of the hollow fiber support in meters;  $l$  the length of the active hollow fiber area in meters; and  $m$  the mass of the permeate in kg. Note that the density of the permeate is taken as 1 kg/L, which is approximately the density of water.

**Salt Retention.**  $\text{MgSO}_4$  salt was used to determine the divalent ion retention of the membranes.  $\text{MgSO}_4$  was dissolved into Milli-Q water to create a 5 mM solution, which was used as feed. The retention was determined by measuring the conductivity of the feed solution halfway through the measurement and that of the permeate after the measurement using a WTW TetraCon 325 conductometer. The retention was calculated according to eq 3.<sup>36</sup>

$$Re = 1 - \frac{C_p}{C_f} \times 100\% \quad (3)$$

Here,  $Re$  is the retention of the sample;  $C_p$  is the salt concentration of the permeate; and  $C_f$  is the concentration of the feed.

**Molecular Weight Cutoff.** MWCO measurements were performed with a feed solution containing 1 g/L of different PEGs with molecular weights of 200, 400, 1000, 1500, 2000, 3000, 4000, 6000, and 10 000 g/mol in Milli-Q water. The membranes were operated in the cross-flow configuration under the same conditions as mentioned above. Gel permeation chromatography (GPC; Agilent 1200/1260 Infinity GPC/SEC series, Polymer Standards Service data center and column compartment) over two Polymer Standards Service Suprema 8 × 300 mm columns in series (1000 Å, 10 μM; 30 Å, 10 μM) was used to analyze the retention of the different solutes. GPC analysis was performed on the permeate and on a sample of the feed solution taken halfway through the experiment. For the GPC measurement, an aqueous solution containing 50 mg/L  $\text{NaN}_3$  was used as the eluent. The retention was then determined using eq 3. To obtain the MWCO, the data were interpolated to find the molecular weight at which 90% was retained.

**Scanning Electron Microscopy.** The layer thickness of the lignin PEMM was studied by using scanning electron microscopy (SEM). To prepare the samples, the membranes were left overnight in a solution of IPA. The cross-sections were prepared by fracturing the membranes after freezing them in liquid nitrogen. Next, the membranes were dried in a vacuum oven at 30 °C overnight, after which they were coated with a 5 nm layer of Pt/Pd using a Quorum Q150T ES (Quorum Technologies, Ltd., UK) sputter coater. The images were captured using a Jeol SEM JSM 7610F field emission scanning electron microscope.

**Salt Stability.** To investigate the saline stability, NaCl solutions with concentrations of 300 600, 1, 1.5, 2, 3, and 5 M were made. Membranes with 9.5 and 10.0 bilayers of lignin were treated with the solutions in order of increasing salinity by leaving them overnight in the solutions. The pure water permeability of the membranes was measured before and after each treatment step. Furthermore, the MWCO and  $\text{MgSO}_4$  retentions were determined before the first treatment and after the 5 M NaCl treatment step. Before the measurements, the membranes were rinsed with pure water until the conductometer could not detect any conductivity, resulting from NaCl, in the retentate stream. Between and after the measurements, the liquid inside the module was removed so as to not alter the concentration of the salt solutions and the permeability of the measurements significantly. As drying the membranes could cause the pores of the support to collapse under the capillary pressure, a reference batch of membranes was measured. These membranes were made and treated in the exact same way, except that they were left overnight in pure Milli-Q water instead of NaCl solutions to

determine if removing the liquid from the modules would affect the integrity of the membrane.

**pH Stability.** To test the pH stability, solutions with different pH values were made by adding HCl or NaOH to Milli-Q water. Solutions with pH values of 1, 2, 3, 4, 5, 9, 10, 11, and 12 were made. Membranes with 9.5 and 10.0 bilayers of lignin were treated with either the acidic or basic solutions in order of increasing acidity or basicity. The pure water permeability was measured before and after each treatment step, and the  $\text{MgSO}_4$  retention and MWCO were measured before and after the sequence of treatments. The data were compared to those of the same reference membranes of the salt stability tests in order to be able to account for the possible collapse of the pores through drying.

**Biodegradability Tests.** To assess the biodegradability of the membranes, the procedure of Pan et al.<sup>37</sup> was adapted. Membranes were fabricated with 9.5 and 10.0 bilayers of lignin and stored in a 0.1 M acetate buffer solution at pH 4.6 containing 0.5 U/mL of laccase and 0.25 mM ABTS. The solution was kept in a climate control system (WTW TS606/2-i) at 40 °C for 3 weeks. During this time, the solution was exposed to air within the chamber to maintain an oxygen supply for the enzymes. The water that evaporated from the solution during the experiment was replaced to maintain the pH and concentration of the solution. As a reference, a second batch of 9.5 and 10.0 lignin bilayer membranes was stored in the same acetate buffer solution, only without laccase and ABTS, and kept under the same conditions. To determine if the laccase was capable of degrading the lignin membranes, the pure water permeability,  $\text{MgSO}_4$  retention, and MWCO of the membranes were measured before and after the treatments.

## RESULTS AND DISCUSSION

**Characterization of the Lignin PEMM Properties.** The amount of lignin bilayers needed to close the pores of the support membrane had to be determined in order for us to be able to study the properties of lignin PEMs. This corresponds to the PEMM transitioning from the pore-dominated regime to the layer-dominated regime.<sup>38</sup> To determine this point, the odd–even effect was used. This effect is a collective term referring to the difference in properties, caused by a difference in swelling between PEMs terminated with either positively or negatively charged polyelectrolytes. Generally, a switch in the odd–even effect is observed when enough bilayers have been adsorbed to reach the layer-dominated regime,<sup>38</sup> which coincides with a large increase in retention and decrease in permeability. To study this effect, PEMMs were fabricated with different numbers of bilayers coated onto the support membranes and their permeability and  $\text{MgSO}_4$  retention were measured.

The results (Figure 2a) show that across the range of 0.5–10.0 bilayers, no switch in the odd–even effect was observed in combination with a large decrease in permeability or large increase in  $\text{MgSO}_4$  retention. However, the permeability did show a steep decline up until 5.5 bilayers, at which point it leveled off. Similarly, the  $\text{MgSO}_4$  retention showed an increase up until 5.5 bilayers, after which it also leveled off. Due to this leveling off of both the permeability and  $\text{MgSO}_4$  retention at the same point, we assume that the pores of the support membrane closed at 5.5 bilayers. The absence of a clear switch in the odd–even effect might be due to a very open structure of the lignin-based membranes, causing the transition from the pore-dominated regime to the layer-dominated regime to not be observed in the odd–even effect.

The statement that the pores of the support membrane were closed after 5.5 bilayers is further supported by the fixed-angle reflectometry data. Using the Q-factors determined by the refractive index measurements (Supporting Information S2), it

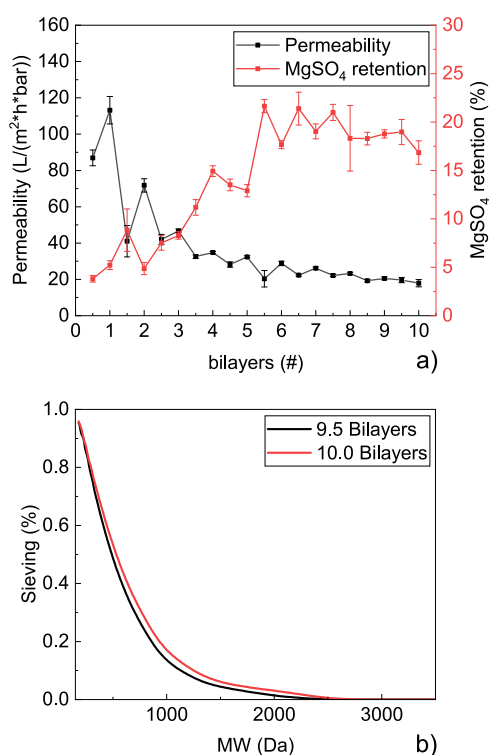


**Figure 2.** (a) Permeability and MgSO<sub>4</sub> retention measured at different amounts of bilayers. The error bars indicate the standard deviation ( $N = 4$ ); (b) sieving curves of the 9.5 and 10.0 bilayer membranes measured.

was calculated that 11.0 mg/m<sup>2</sup> of polyelectrolyte absorbs to the silica substrate in 5.0 bilayers in the case of 50 mM NaCl in the coating solution (Figure 3a). Comparing this with results of different PEM systems previously studied in our group, it can be seen that the lignin absorbs more than other PEM systems such as the polydiallyldimethylammonium chloride/polystyrenesulfonate (PDADMAC/PSS) system, which absorbs 5.7 mg/m<sup>2</sup> under similar conditions. This system, when coated onto the same support membranes as the lignin PEM, is capable of closing the pores in 7 bilayers under the same coating conditions.<sup>38</sup> We believe it is therefore reasonable to assume that the pores for the substrate have closed and the system is in the layer-dominated regime.

To determine the layer thickness of the PEM, SEM images were taken of the bare support membrane and the coated membranes (Supporting Information S3). From the cross-sectional images, no clear distinction can be made between the images of the bare support layer and the coated membranes. However, when looking at the surface images, a clear change in the morphology of the surface can be seen for both the 9.5 and 10.0 bilayer membranes, indicating that lignin is absorbing to the support. The fact that no difference can be observed in the cross-sectional images thus indicates that the thickness of the coating is smaller than that visible on the SEM image, indicating that it is smaller than 100 nm.

To investigate if the PEM forms a homogeneous layer without defects, the sieving curves of the 9.5 bilayer and 10.0 bilayer membranes were measured. In the case of defects, PEG sieving curves tend to show a retention that does not reach 0% or a shoulder in the curve, indicating that defects are letting

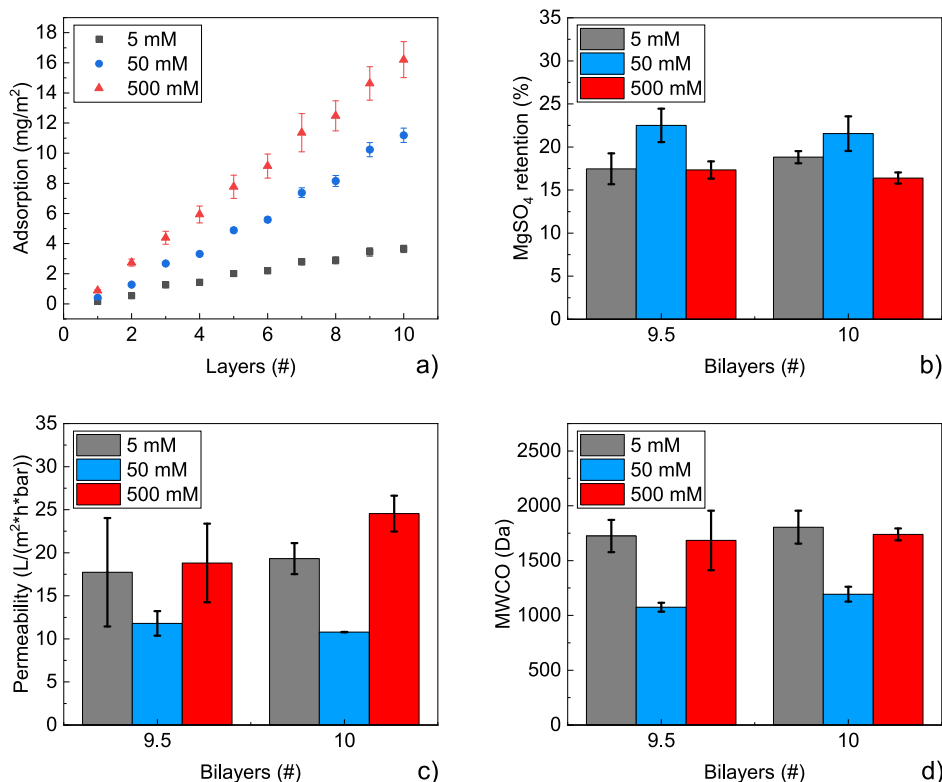


**Figure 3.** Results of the membranes coated with different concentrations of NaCl in the polyelectrolyte coating solutions: (a) reflectometry results showing the adsorption of lignin to a negatively charged silica waver, where the first monolayer adsorbed is PEI; (b) MgSO<sub>4</sub> retention of the membranes; (c) pure water permeability; (d) MWCO. The error bars in the graphs indicate the standard deviation [ $N = 4$  for (b–d) and  $N = 3$  for (a)].

through some larger solutes<sup>39</sup> (see Supporting Information S4 for an example). The 9.5 and 10.0 bilayer membranes were chosen as we were confident that for this amount of bilayers, the pores in the support membrane would be closed. This would then cause slight variations in the coating conditions to not immediately result in open pores of the support, which could then be seen as defects.

Looking at the sieving curves of the 9.5 and 10.0 bilayer membranes, a clear trend with no shoulders in the curve (Figure 2b) can be seen. Furthermore, both curves reach a sieving value of 0%, indicating that no defects are present in the membrane and a homogeneous layer is obtained.

In addition to determining the presence of a homogeneous layer, the sieving curves were used to determine the MWCO of the membranes. The MWCOs were determined to be  $1159 \pm 34$  and  $1324 \pm 105$  Da for the 9.5 and 10.0 bilayer membranes, respectively, indicating that the lignin forms a NF membrane. These results are also in line with the high permeability of 20 L/(m<sup>2</sup> × h × bar) and low MgSO<sub>4</sub> retention of 19% observed (Figure 2). The results thus clearly indicate that the lignin polyelectrolytes are capable of forming a PEMM with separation properties resembling those of loose NF membranes. Comparing these results to the results of synthetic PEMs (see Table 1), it becomes clear that the lignin PEMs form more open membranes, which is likely caused by the more stiff nature and the lower charge density of the lignin.<sup>40,41</sup> They have the advantage of higher permeability in combination with lower divalent ion retention, avoiding the formation of concentrated brines. However, they come with the cost of a higher MWCO. The high MWCO means that they are not suitable for the removal of organic micropollutants, an application that the synthetic PEMMs are mostly used for;<sup>39,42</sup> however, they are still suitable for the separation of NOMs.<sup>2</sup> Moreover, on comparing the results of our all-lignin PEMMs to the results of other PEMMs that used lignin as a polyelectrolyte, our membranes show much lower MWCOs and divalent ion retentions while having similar permeabilities. Our all-lignin PEMMs clearly form an improvement over PEMMs in which only one of the polyelectrolytes is lignin. Furthermore, comparing the results of our lignin PEMMs to that of commercial NF membranes with similar MWCOs (Table 2) shows that our lignin PEMMs display a high permeability for the MWCO that they have. These results thus highlight the potential for lignin PEMMs as a high-permeability, loose nanofiltration membrane.

As a final note on the properties of the membranes, the reproducibility of the membranes was investigated by comparing the data of the membranes made from different cationic lignin batches (Supporting Information S5). From these results, it can clearly be observed that the MWCO and MgSO<sub>4</sub> retentions are not influenced by the different batches of cationic lignin. However, the permeability of the membranes can vary from 22.9 to 11.8 L/m<sup>2</sup> × h × bar. The reason for this could be a change in the charge density of the cationic lignin, resulting in a membrane with more or less polar regions in the lignin resulting in more or less affinity to water. From these results, it can thus clearly be seen that membranes with reproducible retentions can be made; however, the synthesis of the cationic lignin must be performed in a more controlled manner to obtain reproducible permeabilities.

**Influence of Salt Concentration in the Coating Solution on Membrane Properties.** An advantage of PEMMs is that their properties can be fine-tuned by the

**Table 1. Comparison of Different PEMM Properties with That of the Lignin PEMMs; \*Poly(allylamine hydrochloride); \*\*Polyacrylic Acid; \*\*\*Poly(4-aminostyrene); \*\*\*\*Kraft Lignin; \*\*\*\*\*Lignosulfonate**

polyelectrolyte pair	coating conditions	measuring conditions	PWP [L/(m <sup>2</sup> × h × bar)]	MgSO <sub>4</sub> retention	MWCO (g/mol; PEG)	source
PAH*/PSS	dip-coating, 8 bilayers, HF, 0.1 g/L polyelectrolyte, 0.05 M NaCl, pH 6	cross-flow, 5 bar, 1.1 m/s cross-flow velocity	12.8 ± 0.8	>95%	264 ± 7	35
PDADMAC/PAA**	dip-coating, 8 bilayers, HF, 0.1 g/L polyelectrolyte, 0.05 M NaCl, pH 6	cross-flow, 5 bar, 1.1 m/s cross-flow velocity	2.7 ± 0.2	≈10%	316 ± 10	35
PDADMAC/PSS	dip-coating, 8 bilayers, HF, 0.1 g/L polyelectrolyte, 0.05 M NaCl, pH 6	cross-flow, 5 bar, 1.1 m/s cross-flow velocity	12.1 ± 0.6	>95%	283 ± 4	35
PAH*/PAA**	dip-coating, 8 bilayers, HF, 0.1 g/L polyelectrolyte, 0.05 M NaCl, pH 6	cross-flow, 5 bar, 1.1 m/s cross-flow velocity	1.3 ± 0.06	≈80%	185 ± 14	35
PEI/PSS	dip-coating, 10 bilayers, HF, 0.1 g/L polyelectrolyte, 0.05 M NaCl, pH 2 for PSS and pH 5.5 for PEI	cross-flow, 1 m/s cross-flow velocity, 6.2 bar for MgSO <sub>4</sub> and permeability, 2 bar for MWCO	4	>95%	239	42
PAS***PSS	dip-coating, 10 bilayers, HF, 0.1 g/L polyelectrolyte, 0.05 M NaCl, pH 2 for PSS and pH 5.5 for PAS***	cross-flow, 1 m/s cross-flow velocity, 6.2 bar for MgSO <sub>4</sub> and permeability, 2 bar for MWCO	22	≈70%	713	42
PEI/LS*****/PAH*/LS*****	brush-assisted LBL deposition, 2 bilayers, flat sheet, 2 g/L for LS and PAH*, 1 g/L for PEI, GA cross-linked, DI water	cross-flow, 10 bar		≈40%	≈1750	29
PDADMAC/KL*****	static coating, 3 bilayers, flat sheet, 20 g/L polyelectrolyte, DI water, pH 7	dead-end, 4.8 bar initial pressure for MWCO, 2.1 bar pressure for PWP	23		2000	30
cationic KL*****/LS*****	dip-coating, 9.5 bilayers, HF, 0.1 g/L polyelectrolyte, 0.05 M NaCl, pH 6	cross-flow, 2 bar	20 ± 1.4	19 ± 1.4	1159 ± 34	this work

Table 2. Comparison of the Lignin PEMMs with Different Types of Commercial NF Membranes with Similar MWCOs<sup>a</sup>

membrane	membrane material	manufacturer	permeability [L/(m <sup>2</sup> × h × bar)]	MWCO	source
NFPES10	hydrophilic PES support	Nadir	15.4	1200	43
NF80	SPES* support PEM coating	NX Filtration	7.2 ± 0.1	800	44
Sepro NF 6	polyamide coating	Ultura	14.1 ± 0.8	860	45
HFW 1000	SPES* support PEM coating	Pentair X-flow	10	1000	46
lignin PEMM	SPES* support lignin PEM coating		20 ± 1.4	1159 ± 34	this work

<sup>a</sup>\*Sulfonated polyethersulfonate.

ionic strength of the coating solutions.<sup>38</sup> A higher ionic strength leads to screening of the polyelectrolyte ionic groups, resulting in ion–polyelectrolyte interactions called extrinsic charge-compensated interactions. Due to these hydrated ions entering the PEM, the layer swells, resulting in a PEMM with higher permeabilities but lower retentions.<sup>38,47,48</sup>

To study the effect of the ionic strength of the coating solution on the PEMM properties, the layer growth of lignin was studied under different coating conditions. The reason for this is that an increase in ionic strength is known to grow thicker PEMs.<sup>38,48</sup> Therefore, changing the ionic strength will result in more or less lignin absorbing to the support membrane. Thus, a different number of bilayers will be needed to close the pores of the support.

To study the growth of the layers, reflectometry was used with solutions containing 5, 50, and 500 mM NaCl (Figure 3a). The results show that the lignin had a linear growth profile for each of the different NaCl concentrations used. The results were in line with the literature showing that the solutions with the highest NaCl concentration, and thus the highest ionic strength, adsorbed the most lignin.<sup>38,48</sup>

The membrane properties of the lignin PEMMs coated from different ionic strengths (Figure 3b–d) show mixed results with both the 5 and 500 mM membranes having a higher permeability and lower selectivity than the 50 mM membranes, indicating the formation of a more open PEMM. These results can be explained by the fact that both the layer thickness and the dominant type of charge compensation change with a change in the ionic strength. The increase in permeability and decrease in selectivity from the 50 toward the 500 mM coating solution can be explained by the charge compensation transitioning from intrinsic to more extrinsic, leading to the formation of a more open PEMM. The decrease in permeability and increase in selectivity while going from the 5 mM coating solution to the 50 mM coating solution is, however, caused by the decrease in adsorption of the lignin. As was previously shown from the reflectometry data in Figure 3a and the permeability and retention data in Figure 2a, the 50 mM PEM adsorbed 11 mg/m<sup>2</sup> in 5 bilayers and was able to close the pores of the support in 5.5 bilayers. As the 500 mM PEM adsorbed more lignin, it is reasonable to assume that it is capable of closing the pores of the substrate within 5.5 bilayers. However, for the 5 mM case, less lignin adsorbs, indicating that more bilayers will be needed to close the pores of the support. The 5 mM PEM was able to adsorb 3.6 mg/m<sup>2</sup> in 5 bilayers. Therefore, assuming that 15 mg/m<sup>2</sup> would be enough to close the pores and avoid the formation of any defects, 21 bilayers would be needed to close the pores of the support. As for the sake of comparison, only 9.5 and 10.0 bilayer PEMMs were made, the 5 mM PEMMs are most likely still in the pore-dominated regime. This causes them to appear to have formed a more open PEMM, while, in fact, the PEM itself is most likely more dense due to the intrinsic charge compensation.

These results thus indicate that the properties of the lignin PEMM can be fine-tuned by changing the ionic strength of the coating solutions to form a denser or more open PEMM.

**Salt Stability.** A known issue with PEMMs is their poor stability against saline solutions.<sup>49</sup> As solutions of high ionic strength are capable of screening the ionic charge of the polyelectrolytes, the PEMs are expected to release at high salt concentrations due to being extrinsically charge-compensated.<sup>47,49–51</sup> To test the stability of the lignin PEMM against saline solutions, the membranes were exposed to NaCl solutions of different concentrations, and their separation properties were measured before and after exposure. A reference sample was also studied that was not exposed to high salt concentrations but was treated with the same drying and wetting steps.

Looking at the results of the salt stability experiments (Figure 4), one can see that the reference sample remained relatively stable over the course of the experiment. This indicates that the drying and wetting of the membrane did not induce significant collapse of the porous structure of the membrane due to capillary pressures. The fluctuations seen in the measurements can simply be attributed to slight fluctuations in experimental parameters, such as pressure, temperature of the feed, and flow.

In the case of the NaCl-treated membranes (Figure 4), it can be seen that the pure water permeability does not increase significantly during the treatments (Figure 4a). Even though a slight increase in permeability is observed compared with the reference measurement, all data points fall within each other's margin of error. Looking at the MgSO<sub>4</sub> retention and MWCO, however, a decrease in MgSO<sub>4</sub> retention and increase in MWCO can be observed (Figure 4b,c, respectively). These results indicate that a more open PEMM has been formed. This is most likely due to some swelling of the membrane caused by the polymer–polymer charge interactions (intrinsic charge interactions) becoming more extrinsically charge-compensated.<sup>47,48</sup> It can therefore be stated that the membranes did not remain fully stable across the entire range up to 5 M. However, much of the lignin did remain adsorbed to the support membrane. This can be seen due to the fact that the pure water permeability and MWCO are still significantly lower than those of the UF hollow fiber support membranes, which have a pure water permeability and MWCO of 142.8 L/(m<sup>2</sup> × h × bar) and 10 kDa, respectively. Comparing this to the work of Han et al.,<sup>51</sup> where a PDADMAC/PSS PEM system was studied, which has the same quaternary ammonium/sulfonate ionic bonds as the lignin PEM system studied in this research, it could be seen that 72% of the mass of the PEM layer desorbs upon treatment with a 5 M NaCl solution. In other work on the PDADMAC/PSS system,<sup>49</sup> similar measurements were performed where the pure water permeability of PDADMAC/PSS membranes was measured after different salt treatments up to 1.5 M. From this

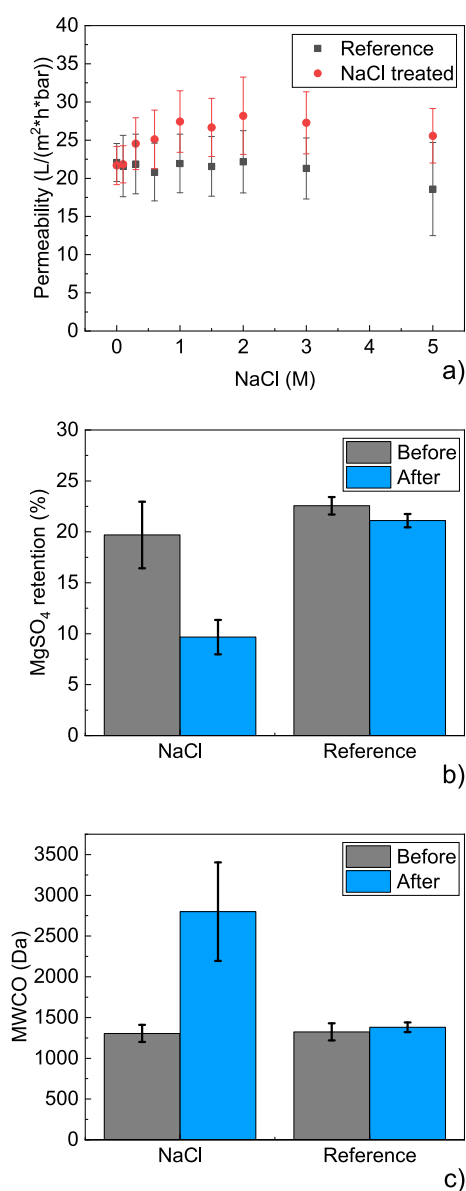


**Figure 4.** Results of the 10.0 bilayer membranes before and after treatment with the entire sequence of salt (NaCl) solutions or drying treatments (reference). The membranes were treated in order of increasing NaCl concentration: (a) pure water permeability; (b) MgSO<sub>4</sub> retention before the 300 mM and after the 5 M NaCl treatments; and (c) MWCO before the 300 mM and after the 5 M NaCl treatments. Error bars indicate the standard deviation ( $N = 4$ ).

work, it was observed that the permeability of the PDADMAC/PSS system remained stable up until 1 M, after which it showed a substantial increase in permeability attributed to the irreversible rearrangement of the multilayer. Next to this, the PDADMAC/PSS system has proven to form very stable ionic bonds compared to other PEM systems.<sup>50</sup> The fact that the lignin PEM system was capable of retaining a permeability of 25.6 L/(m<sup>2</sup> × h × bar) after a 24 h treatment in 5 M NaCl indicates that it has better stability compared to other systems. The reason for this good stability and the slight decrease in permeability after the 2 M NaCl treatment might be attributed to both the aromatic rings and hydrophobic parts of the lignin. It is known that in lignin, the aromatic rings can form a secondary binding interaction between the different

lignin molecules through  $\pi$ - $\pi$  stacking.<sup>52</sup> These bonds could hold the lignin in place even when the ionic bonds break. In combination with this, the hydrophobic parts of the lignin will most likely form hydrophobic regions in the multilayer to avoid contact with water.<sup>18</sup> To fully reverse the lignin complexation, these hydrophobic groups would need to redissolve in water. This is, however, unfavorable, providing the multilayer with an extra energy barrier that needs to be overcome to redissolve the lignin. The results of the 9.5 bilayer membranes showed a similar but slightly weaker trend to those of the 10.0 bilayer samples (Supporting Information S6).

**pH Stability.** Another important parameter of membranes is their stability against acids and bases as this provides insights into the applications and cleaning procedures that can be used on the membranes.

To determine the pH range in which the lignin PEMMs were stable, the membranes were left overnight in solutions of increasing or decreasing pH, starting from pure water (pH 7). The reference membranes in the salt stability experiments (Figure 4 and Supporting Information S6) were considered as a reference for these experiments.

The permeability data for the 10.0 bilayer membranes showed that the permeability remained constant for the samples treated with the acidic solutions (Figure 5a). This indicates that the lignin PEMMs remain stable in a pH range from 7 to 1. The MgSO<sub>4</sub> retention (Figure 5b) data support these findings as it does not differ significantly after the treatment with the pH 1 solution. The MWCO data (Figure 5d) show a similar increase to those of the reference samples (Figure 4c), indicating that this increase cannot be attributed to the presence of the acid but was most likely caused by fluctuations in the measurement conditions. The lignin membranes that were treated with the alkaline solutions, however, do show an increase in permeability after treatment with a pH 12 solution (Figure 5c). The MgSO<sub>4</sub> retention and MWCO (Figure 5b,d, respectively) show a decrease and increase, respectively, indicating that the membranes are not stable under these conditions. The MgSO<sub>4</sub> retention of the pH 12 treated membranes shows a drop from 22 to 5.6%, while the MWCO increases to beyond 10 kDa. The exact value of the MWCO for these membranes was not known as the highest MW PEG used in the retention measurement was 10 kDa, which was lower than the MWCO of the membranes. It can, however, be stated that the lignin was nearly completely removed as the MWCO and permeability reached values similar to those of the UF support membrane [10 kDa and 142.8 L/(m<sup>2</sup> × h × bar), respectively, according to the manufacturer]. The instability of the lignin in alkaline conditions is in line with what is reported in the literature as it is known that the  $\beta$ -aryl ether bonds in lignin can be cleaved at ambient temperatures through NaOH.<sup>53</sup> Next to this, the pK<sub>a</sub> of lignin is known to be between 6.2 and 11.3, indicating that at pH 12, all hydroxyl groups in the lignin are deprotonated.<sup>54</sup> The increase in anionic groups might also start to repel the lignosulfonates from the now zwitterionic Kraft lignin, causing them to redissolve. The results of the 9.5 bilayer membranes (Supporting Information S7) show a trend similar to those of the 10.0 bilayer membranes, indicating that the stability is independent of the charge of the final layer.

From the pH stability results, it can thus be concluded that the lignin PEMMs show good stability over the pH range of 1–11. Applications and membrane cleaning protocols that fall



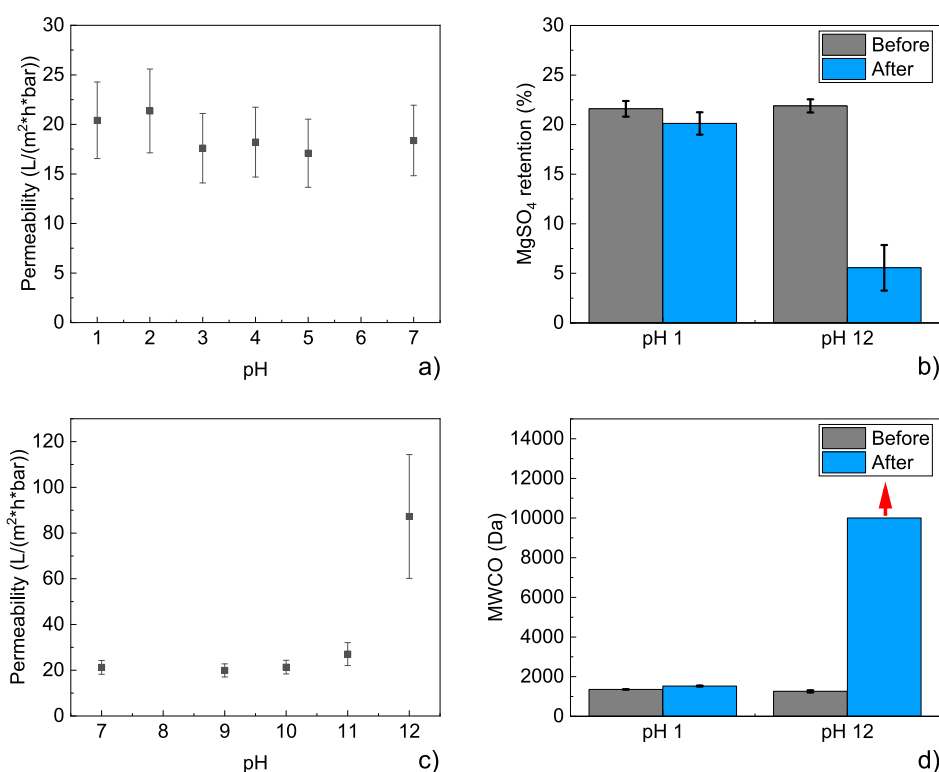


**Figure 5.** pH stability tests of the 10.0 bilayer lignin PEMMs: (a) pure water permeability of the membranes treated in the acidic pH range. The membranes were treated in sequence from pH 7 to 1; (b) MgSO<sub>4</sub> retention of the membranes before and after treatment with the entire sequence of either the acid or base solutions; (c) pure water permeability of the membranes treated with alkaline solutions. The membranes were treated in sequence from pH 7 to pH 12; (d) MWCO of the membranes before and after treatment with the entire sequence of either the acid or base solutions. For the pH 12 sample, the MWCO was higher than the MW of the PEGs used. Therefore, it could not be measured. The value displayed is the value of the highest MW of PEG used in the measurement. The red arrow indicates that the MWCO is larger than this value. The error bars in the graphs indicate the standard deviation ( $N = 4$ ).

within this range of operation can thus safely be used for these all-lignin membranes.

**Biodegradability of the Lignin PEMMs.** To investigate the biodegradability of the all-lignin PEMMs, the 9.5 and 10.0 bilayer membranes were treated with a laccase/ABTS enzyme/mediator solution.

Upon addition of the ABTS to the laccase solution, the solution turned a dark blue color, indicating that the laccase was active. During the course of the treatments, the blue color of the solution faded, indicating that the activated ABTS was reacting and the enzymes were losing their activity during the course of the experiment.

On comparing the results of the 10.0 bilayer membranes before and after laccase treatment (Figure 6), an increase in permeability and MWCO can be seen in combination with a decrease in MgSO<sub>4</sub> retention in the case of a buffer treatment. This indicates that the membranes became more open. This can be explained due to the ionic strength of the buffer solution, causing the ionic bonds of the membranes to go from more intrinsic to more extrinsic, creating a more open PEMM as was observed in the saline stability experiments performed (Figure 4).<sup>47–49,51</sup> However, for the case of the laccase treatment, the permeability and MWCO showed a much larger increase in combination with a larger decrease in the MgSO<sub>4</sub> retention. This indicates that the all-lignin membranes had been degraded by the treatment with the laccase enzymes. The lignin had, however, not been fully removed from the substrate as the permeability, which was 36 L/(m<sup>2</sup> × h × bar), was still significantly lower than that of the bare substrate, which was

142.8 L/(m<sup>2</sup> × h × bar). The extent of degradation might, however, be more pronounced than seen in the results, as laccase/ABTS can be seen fouling the membrane (Supporting Information S8). The MWCO after the treatment was similar to that of the support membranes as reported by the supplier (10 kDa). This high MWCO in combination with the still low permeability can be understood by the PEMM having large defects caused by the degradation. These defects increase the MWCO without fully removing the lignin in its entirety from the substrate. For the case of the 9.5 bilayer samples, similar results were obtained (Supporting Information S9). It can thus be concluded that the membranes retained their biodegradable properties.

As a final note, the authors discuss the lifetime of lignin PEMMs in operation. Biofouling often occurs during the operation of membranes<sup>55</sup> and might cause the lignin membranes to degrade at undesired moments. We, however, believe this problem to be limited. The reasons for this are that biofouling is mainly caused by bacteria algae and other small organisms.<sup>56</sup> Fungi are not predominant in these types of streams due to the specific pH conditions needed for fungi to thrive.<sup>57</sup> Thus, only specific bacteria are able to degrade lignin in aqueous streams,<sup>18,25–27</sup> and bacteria degrade lignin at a slower rate than the fungi.<sup>57</sup> Furthermore, modified lignin such as Kraft lignin and lignosulfonates degrade slower than natural lignin.<sup>28</sup> The cationic Kraft lignin has undergone even further modifications, which most likely slow down the degradation process even more. Additionally, the ionic cross-links in the PEMM decrease the accessibility of the enzymes to the lignin

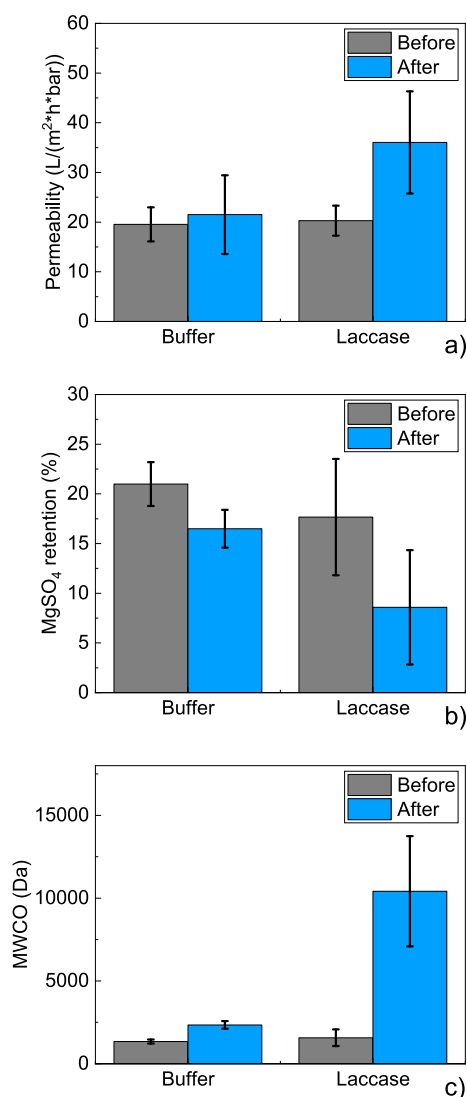


**Figure 6.** Measurements of the 10.0 bilayer membranes before and after the enzyme (laccase) and reference (buffer) treatment: (a) pure water permeability; (b) MgSO<sub>4</sub> retention; (c) MWCO. Error bars indicate the standard deviation ( $N = 4$ ).

through forming a dense network. Next to this, it has also been shown that lignin degradation is slower in aqueous environments.<sup>28</sup> Finally, the biodegradability experiments in this work were performed with enzyme concentrations an order of magnitude higher than those that would occur in natural environments to speed up the degradation process. The three-week timespan is therefore not representative of the actual natural degradation rate. We therefore believe it to be reasonable to assume that the lignin PEMMs would provide a proficient lifetime during operation. The results that are presented above, however, do show that under the right conditions, the lignin can still be biodegraded, highlighting a good balance between stability and degradability when desired. We, however, acknowledge that this claim must be further investigated in the future through lifetime tests with real wastewater.

## CONCLUSIONS

We were able to fabricate the first all-lignin PEMM by using lignosulfonates in combination with synthesized cationic

lignins as a membrane material. The all-lignin PEMMs showed separation properties corresponding to loose NF membranes. Such open NF membranes are normally not reported based on synthetic PEMs. This makes lignin PEMMs the ideal candidates for the removal of larger pollutants, such as NOMs, while avoiding the creation of concentrated brines. We demonstrated that the properties of the lignin PEMMs could easily be modified by changing the ionic strength of the coating solution, proving that the lignin PEMMs could be tailored to suit different applications. Furthermore, the lignin PEMMs are unique in showing good physical and chemical stability while retaining their biodegradable properties when exposed to specific enzymes. We showed that the membranes were stable over a pH range of 1–11 and had stability in saline solutions beyond that of PEMMs made with synthetic polymers. These results thus highlight that lignin allows new types of PEMMs to be formed with separation properties and stabilities not seen before in synthetic PEMMs, adding to the already large versatility of this type of membrane. Furthermore, our results prove that an active separation layer with desirable properties can be fabricated from a bio-based and biodegradable polymer. However, it must be noted that the PES substrate used in this work is not biodegradable, which should be seen as a logical next step. This research can therefore be seen as a step toward building a biodegradable NF membrane in which both the separation layer and support are made from bio-based and biodegradable materials for aqueous separations.

## ASSOCIATED CONTENT

### Supporting Information

The Supporting Information is available free of charge at <https://pubs.acs.org/doi/10.1021/acsapm.3c01661>.

Lignin characterization, Q-factor determination for reflectometry, SEM images of the lignin-coated HF, sieving curves of membranes containing defects, comparison of membrane properties between the different cationic lignin batches, image showing the membrane discoloration caused by the laccase ABTS treatment, and results of the positively terminated PEMMs (PDF)

## AUTHOR INFORMATION

### Corresponding Authors

**Frederik R. Wurm** – Sustainable Polymer Chemistry Group  
Department of Molecules & Materials MESA+ Institute of Nanotechnology, University of Twente, Enschede 7500AE, The Netherlands; [orcid.org/0000-0002-6955-8489](https://orcid.org/0000-0002-6955-8489);  
Email: [frederik.wurm@utwente.nl](mailto:frederik.wurm@utwente.nl)

**Wiebe M. de Vos** – Membrane Surface Science Membrane Science and Technology MESA+ Institute of Nanotechnology, University of Twente, Enschede 7500AE, The Netherlands; [orcid.org/0000-0002-0133-1931](https://orcid.org/0000-0002-0133-1931); Email: [w.m.devos@utwente.nl](mailto:w.m.devos@utwente.nl)

### Authors

**Tjerk R. Watt** – Membrane Surface Science Membrane Science and Technology MESA+ Institute of Nanotechnology, University of Twente, Enschede 7500AE, The Netherlands

**Stefan Peil** – Sustainable Polymer Chemistry Group  
Department of Molecules & Materials MESA+ Institute of Nanotechnology, University of Twente, Enschede 7500AE, The Netherlands

Wendy A. Jonkers – Membrane Surface Science Membrane Science and Technology MESA+ Institute of Nanotechnology, University of Twente, Enschede 7500AE, The Netherlands; [orcid.org/0000-0003-3308-5111](https://orcid.org/0000-0003-3308-5111)

Jurjen A. Regenspurg – Membrane Surface Science Membrane Science and Technology MESA+ Institute of Nanotechnology, University of Twente, Enschede 7500AE, The Netherlands

Complete contact information is available at:  
<https://pubs.acs.org/10.1021/acsapm.3c01661>

## Notes

The authors declare no competing financial interest.

## REFERENCES

- (1) Sillanpää, M. *Natural Organic Matter in Water*; Butterworth-Heinemann, 2015; pp 1–15.
- (2) Köhler, S. J.; Lavonen, E.; Keucken, A.; Schmitt-Kopplin, P.; Spanjer, T.; Persson, K. Upgrading coagulation with hollow-fibre nanofiltration for improved organic matter removal during surface water treatment. *Water Res.* **2016**, *89*, 232–240.
- (3) Winter, J.; Barbeau, B.; Bérubé, P. Nanofiltration and Tight Ultrafiltration Membranes for Natural Organic Matter Removal-Contribution of Fouling and Concentration Polarization to Filtration Resistance. *Membranes* **2017**, *7*, 34.
- (4) Evans, C. D.; Monteith, D. T.; Cooper, D. M. Long-term increases in surface water dissolved organic carbon: Observations, possible causes and environmental impacts. *Environ. Pollut.* **2005**, *137*, 55–71.
- (5) de Wit, H. A.; Mulder, J.; Hindar, A.; Hole, L. Long-Term Increase in Dissolved Organic Carbon in Streamwaters in Norway Is Response to Reduced Acid Deposition. *Environ. Sci. Technol.* **2007**, *41*, 7706–7713.
- (6) Hongve, D.; Riise, G.; Kristiansen, J. F. Increased colour and organic acid concentrations in Norwegian forest lakes and drinking water – a result of increased precipitation? *Aquat. Sci.* **2004**, *66*, 231–238.
- (7) Sewerin, T.; Elshof, M. G.; Matencio, S.; Boerrigter, M.; Yu, J.; de Grooth, J. Advances and Applications of Hollow Fiber Nanofiltration Membranes: A Review. *Membranes* **2021**, *11*, 890.
- (8) Lidén, A.; Lavonen, E.; Persson, K. M.; Larson, M. Integrity breaches in a hollow fiber nanofilter – Effects on natural organic matter and virus-like particle removal. *Water Res.* **2016**, *105*, 231–240.
- (9) Shan, L.; Liang, Y.; Prozorovska, L.; Jennings, G. K.; Ji, S.; Lin, S. Multifold Enhancement of Loose Nanofiltration Membrane Performance by Intercalation of Surfactant Assemblies. *Environ. Sci. Technol. Lett.* **2018**, *5*, 668–674.
- (10) Joseph, N.; Ahmadiannamini, P.; Hoogenboom, R.; Vankelecom, I. F. J. Layer-by-layer preparation of polyelectrolyte multilayer membranes for separation. *Polym. Chem.* **2014**, *5*, 1817–1831.
- (11) Abtahi, S. M.; Ilyas, S.; Joannis Cassan, C.; Albasi, C.; de Vos, W. M. Micropollutants removal from secondary-treated municipal wastewater using weak polyelectrolyte multilayer based nanofiltration membranes. *J. Membr. Sci.* **2018**, *548*, 654–666.
- (12) Barbosa, M. O.; Moreira, N. F.; Ribeiro, A. R.; Pereira, M. F.; Silva, A. M. Occurrence and removal of organic micropollutants: An overview of the watch list of EU Decision 2015/495. *Water Res.* **2016**, *94*, 257–279.
- (13) Durmaz, E. N.; Sahin, S.; Virga, E.; de Beer, S.; de Smet, L. C. P. M.; de Vos, W. M. Polyelectrolytes as Building Blocks for Next-Generation Membranes with Advanced Functionalities. *ACS Appl. Polym. Mater.* **2021**, *3*, 4347–4374.
- (14) Jonkers, W. A.; Cornelissen, E. R.; de Vos, W. M. Hollow fiber nanofiltration: From lab-scale research to full-scale applications. *J. Membr. Sci.* **2023**, *669*, 121234.
- (15) Hernández-Rivas, M.; Guzmán, E.; Fernández-Peña, L.; Akanno, A.; Greaves, A.; Léonforte, F.; Ortega, F. G.; G Rubio, R.; Luengo, G. S. Deposition of Synthetic and Bio-Based Polycations onto Negatively Charged Solid Surfaces: Effect of the Polymer Cationicity, Ionic Strength, and the Addition of an Anionic Surfactant. *Colloids Interfaces* **2020**, *4*, 33.
- (16) Feig, V. R.; Tran, H.; Bao, Z. Biodegradable Polymeric Materials in Degradable Electronic Devices. *ACS Cent. Sci.* **2018**, *4*, 337–348.
- (17) Dong, X.; Lu, D.; Harris, T. A. L.; Escobar, I. C. Polymers and Solvents Used in Membrane Fabrication: A Review Focusing on Sustainable Membrane Development. *Membranes* **2021**, *11*, 309.
- (18) Huang, J.; Fu, S.; Gan, L. *Lignin Chemistry and Applications*; Elsevier Science, 2019.
- (19) Tao, J.; Li, S.; Ye, F.; Zhou, Y.; Lei, L.; Zhao, G. Lignin – An underutilized, renewable and valuable material for food industry. *Crit. Rev. Food Sci. Nutr.* **2020**, *60*, 2011–2033.
- (20) Scarica, C.; Suriano, R.; Levi, M.; Turri, S.; Griffini, G. Lignin Functionalized with Succinic Anhydride as Building Block for Biobased Thermosetting Polyester Coatings. *ACS Sustainable Chem. Eng.* **2018**, *6*, 3392–3401.
- (21) Peil, S.; Beckers, S.; Fischer, J.; Wurm, F. Biodegradable, lignin-based encapsulation enables delivery of *Trichoderma reesei* with programmed enzymatic release against grapevine trunk diseases. *Mater. Today Bio* **2020**, *7*, 100061.
- (22) Kong, F.; Parhiala, K.; Wang, S.; Fatehi, P. Preparation of cationic softwood kraft lignin and its application in dye removal. *Eur. Polym. J.* **2015**, *67*, 335–345.
- (23) Kai, D.; Tan, M. J.; Chee, P. L.; Chua, Y. K.; Yap, Y. L.; Loh, X. J. Towards lignin-based functional materials in a sustainable world. *Green Chem.* **2016**, *18*, 1175–1200.
- (24) dos Santos, A. C.; Ximenes, E.; Kim, Y.; Ladisch, M. R. Lignin-Enzyme Interactions in the Hydrolysis of Lignocellulosic Biomass. *Trends Biotechnol.* **2019**, *37*, 518–531.
- (25) Datta, R.; Kelkar, A.; Baraniya, D.; Molaei, A.; Moulick, A.; Meena, R. S.; Formanek, P. Enzymatic Degradation of Lignin in Soil: A Review. *Sustainability* **2017**, *9*, 1163.
- (26) Tuomela, M.; Vikman, M.; Hatakka, A.; Itävaara, M. Biodegradation of lignin in a compost environment: a review. *Bioresour. Technol.* **2000**, *72*, 169–183.
- (27) Kumar, A.; Chandra, R. Lignolytic enzymes and its mechanisms for degradation of lignocellulosic waste in environment. *Heliyon* **2020**, *6*, No. e03170.
- (28) Crawford, D. L.; Floyd, S.; Pometto, A. L., III; Crawford, R. L. Degradation of natural and Kraft lignins by the microflora of soil and water. *Can. J. Microbiol.* **1977**, *23*, 434–440.
- (29) Li, Q.; Zhang, N.; Li, Z.; Gao, Z.; Yan, T.; Qian, Z.; Xu, S.; Wang, J. Brush assisted layer-by-layer assembled lignin/polyelectrolyte membrane. *Mater. Lett.* **2021**, *292*, 129650.
- (30) Shamaei, L.; Khorshidi, B.; Islam, M. A.; Sadrzadeh, M. Industrial waste lignin as an antifouling coating for the treatment of oily wastewater: Creating wealth from waste. *J. Cleaner Prod.* **2020**, *256*, 120304.
- (31) Balakshin, M.; Capanema, E. On the Quantification of Lignin Hydroxyl Groups With <sup>31</sup>P and <sup>13</sup>C NMR Spectroscopy. *J. Wood Chem. Technol.* **2015**, *35*, 220–237.
- (32) *The MAK-Collection for Occupational Health and Safety*; John Wiley & Sons, Ltd, 2012; pp 248–255.
- (33) Kolasinska, M.; Krastev, R.; Warszynski, P. Characteristics of polyelectrolyte multilayers: Effect of PEI anchoring layer and posttreatment after deposition. *J. Colloid Interface Sci.* **2007**, *305*, 46–56.
- (34) Virga, E.; Zvab, K.; de Vos, W. M. Fouling of nanofiltration membranes based on polyelectrolyte multilayers: The effect of a zwitterionic final layer. *J. Membr. Sci.* **2021**, *620*, 118793.
- (35) Elshof, M.; de Vos, W.; de Grooth, J.; Benes, N. On the long-term pH stability of polyelectrolyte multilayer nanofiltration membranes. *J. Membr. Sci.* **2020**, *615*, 118532.

- (36) Baker, R. *Membrane Technology and Applications*; John Wiley & Sons, Ltd, 2004; Chapter 2, pp 15–87.
- (37) Pan, Y.; Ma, H.; Huang, L.; Huang, J.; Liu, Y.; Huang, Z.; Li, W.; Yang, J. Graphene enhanced transformation of lignin in laccase-ABTS system by accelerating electron transfer. *Enzyme and Microb. Technol.* **2018**, *119*, 17–23.
- (38) de Grooth, J.; Oborný, R.; Potreck, J.; Nijmeijer, K.; de Vos, W. M. The role of ionic strength and odd–even effects on the properties of polyelectrolyte multilayer nanofiltration membranes. *J. Membr. Sci.* **2015**, *475*, 311–319.
- (39) te Brinke, E.; Reurink, D. M.; Achterhuis, I.; de Grooth, J.; de Vos, W. M. Asymmetric polyelectrolyte multilayer membranes with ultrathin separation layers for highly efficient micropollutant removal. *Appl. Mater. Today* **2020**, *18*, 100471.
- (40) Szabó, G.; Kun, D.; Renner, K.; Pukanszky, B. Structure, properties and interactions in ionomer/lignin blends. *Mater. Des.* **2018**, *152*, 129–139.
- (41) Oveissi, F.; Fatehi, P. Characterization of four different lignins as a first step toward the identification of suitable end-use applications. *J. Appl. Polym. Sci.* **2015**, *132*, 42336.
- (42) Reurink, D. M.; Willott, J. D.; Roesink, H. D. W.; de Vos, W. M. Role of Polycation and Cross-Linking in Polyelectrolyte Multilayer Membranes. *ACS Appl. Polym. Mater.* **2020**, *2*, 5278–5289.
- (43) Boussu, K.; Van der Bruggen, B.; Volodin, A.; Van Haesendonck, C.; Delcour, J.; Van der Meeren, P.; Vandecasteele, C. Characterization of commercial nanofiltration membranes and comparison with self-made polyethersulfone membranes. *Desalination* **2006**, *191*, 245–253.
- (44) Rutten, S. B.; Junker, M. A.; Leal, L. H.; de Vos, W. M.; Lammertink, R. G.; de Grooth, J. Influence of dominant salts on the removal of trace micropollutants by hollow fiber nanofiltration membranes. *J. Membr. Sci.* **2023**, *678*, 121625.
- (45) Ye, W.; Liu, H.; Jiang, M.; Lin, J.; Ye, K.; Fang, S.; Xu, Y.; Zhao, S.; Van der Bruggen, B.; He, Z. Sustainable management of landfill leachate concentrate through recovering humic substance as liquid fertilizer by loose nanofiltration. *Water Res.* **2019**, *157*, 555–563.
- (46) Keucken, A.; Wang, Y.; Tng, K. H.; Leslie, G.; Spanjer, T.; Köhler, S. Optimizing Hollow Fibre Nanofiltration for Organic Matter Rich Lake Water. *Water* **2016**, *8*, 430.
- (47) Schlenoff, J. B.; Dubas, S. T. Mechanism of Polyelectrolyte Multilayer Growth: Charge Overcompensation and Distribution. *Macromolecules* **2001**, *34*, 592–598.
- (48) Ghostine, R. A.; Markarian, M. Z.; Schlenoff, J. B. Asymmetric Growth in Polyelectrolyte Multilayers. *J. Am. Chem. Soc.* **2013**, *135*, 7636–7646.
- (49) de Grooth, J.; Dong, M.; de Vos, W. M.; Nijmeijer, K. Building Polyzwitterion-Based Multilayers for Responsive Membranes. *Langmuir* **2014**, *30*, 5152–5161.
- (50) Virga, E.; de Grooth, J.; Zvab, K.; de Vos, W. M. Stable Polyelectrolyte Multilayer-Based Hollow Fiber Nanofiltration Membranes for Produced Water Treatment. *ACS Appl. Polym. Mater.* **2019**, *1*, 2230–2239.
- (51) Han, L.; Mao, Z.; Wuliyasu, H.; Wu, J.; Gong, X.; Yang, Y.; Gao, C. Modulating the structure and properties of poly(sodium 4-styrenesulfonate)/poly(diallyldimethylammonium chloride) multilayers with concentrated salt solutions. *Langmuir* **2012**, *28*, 193–199.
- (52) Deng, Y.; Feng, X.; Yang, D.; Yi, C.; Qiu, X.  $\pi$ - $\pi$  Stacking of the aromatic groups in lignosulfonates. *Bioresources* **2012**, *7*, 1145–1156.
- (53) Zhang, J.; Zhou, H.; Liu, D.; Zhao, X. *Lignocellulosic Biomass to Liquid Biofuels*; Yousuf, A., Pirozzi, D., Sannino, F., Eds.; Academic Press, 2020; pp 17–65.
- (54) Ragnar, M.; Lindgren, C.; Nilvebrant, N. O. pKa-Values of Guaiacyl and Syringyl Phenols Related to Lignin. *J. Wood Chem. Technol.* **2000**, *20*, 277–305.
- (55) Nguyen, T.; Roddick, F. A.; Fan, L. Biofouling of water treatment membranes: a review of the underlying causes, monitoring techniques and control measures. *Membranes* **2012**, *2*, 804–840.
- (56) de Carvalho, C. C. R. Marine Biofilms: A Successful Microbial Strategy With Economic Implications. *Front. Mar. Sci.* **2018**, *5*, 126.
- (57) Khan, S. I.; Zarin, A.; Ahmed, S.; Hasan, F.; Belduz, A. O.; Çanakçı, S.; Khan, S.; Badshah, M.; Farman, M.; Shah, A. A. Degradation of lignin by *Bacillus altitudinis* SL7 isolated from pulp and paper mill effluent. *Water Sci. Technol.* **2022**, *85*, 420–432.